

Analysis and Design of an Automatic Motion Inverter

Sergio M. Savaresi, *Member, IEEE*, Mara Tanelli, *Member, IEEE*, Francesco L. Taroni, Fabio Previdi, and Sergio Bittanti, *Fellow, IEEE*

Abstract—In this paper, the design of an automatic motion-inverter control system for agricultural tractors has been discussed. The objective of this system is to perform a fully automatic symmetric motion inversion (e.g., from a forward speed of 10 km/h to a reverse speed of -10 km/h). The device used to control the inversion is electro-hydraulic reverser, constituted by two clutches, driven by a proportional electro-hydraulic valve (EVP) and a directional electro-hydraulic valve (EVD). The design of a motion inverter is a nontrivial task, since it is difficult to find a good compromise between speed (the inversion must be completed in a short time) and comfort (bumps and oscillations on the longitudinal speed must be minimized). All the subtasks of the inversion control systems are considered: The design of an inner loop for the control of the EVP current, the open-loop switching strategies, and the design of the outer control loop, which regulates the vehicle speed. The control strategies are experimentally validated, and satisfactory results are obtained.

Index Terms—Agricultural tractors, automotive systems, cascade control, hybrid control, power-shuttle transmission, servo systems.

I. INTRODUCTION AND PROBLEM STATEMENT

IN this paper, the design of an automatic motion-inverter control system for agricultural tractors has been discussed. The objective of this system is to perform a fully automatic symmetric motion inversion (e.g., from a forward speed of 10 km/h to a reverse speed of -10 km/h). The device used to control the inversion is an electro-hydraulic reverser, constituted by two clutches (a forward clutch and a reverse clutch), driven by a Proportional Electro-hydraulic Valve (EVP) and an ON-OFF Directional Electro-hydraulic Valve (EVD).

The control variables are the currents of the EVP and EVD valves and the measured signals are the rotational speeds of the input and output shafts of the reverser.

The design of a motion inverter is a nontrivial task, since it is difficult to find a good compromise between speed (the inversion must be completed in a short time) and comfort (bumps and oscillations on the longitudinal speed must be minimized). This control problem is particularly challenging since the motion-inversion procedure can be activated by the driver under very different working conditions. Specifically, the changes of the tractor inertia, the use of heavy trailers, the presence of road

Manuscript received September 30, 2004; revised January 30, 2006. Recommended by Technical Editor C. Mavroidis. This work was supported by the R&D Department of the SAME Deutz-Fahr Group and by MIUR project “New methods for Identification and Adaptive Control for Industrial Systems.”

S. M. Savaresi, M. Tanelli, and S. Bittanti are with the Dipartimento di Elettronica e Informazione, Politecnico di Milano, 20133 Milano, Italy (e-mail: savaresi@elet.polimi.it; tanelli@elet.polimi.it; bittanti@elet.polimi.it).

F. L. Taroni is with the SAME Deutz-Fahr Group, 24047 Treviglio, Bergamo, Italy (e-mail: Francesco.Taroni@Samedeutz-fahr.com).

F. Previdi is with the Dipartimento di Ingegneria, Università degli Studi di Bergamo, 24044 Dalmine, Bergamo, Italy (e-mail: fabio.previdi@unibg.it).

Digital Object Identifier 10.1109/TMECH.2006.875552

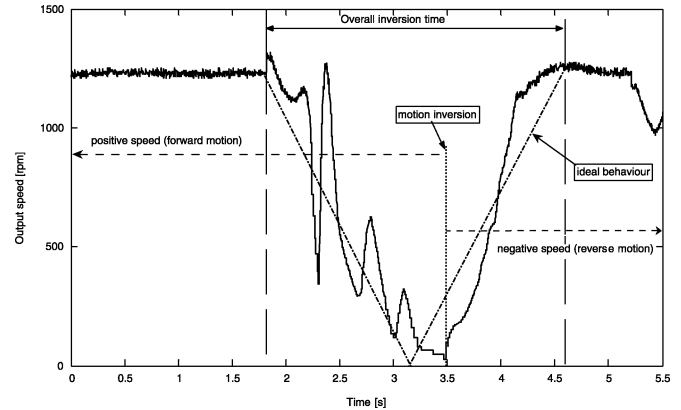


Fig. 1. Output speed of the reverser during a forward \rightarrow reverse inversion.

slopes, and the changes of the working temperature of the reverser are particularly obnoxious. Since all these changes can hardly be detected in practice, an adaptive-control approach is a questionable choice. In this paper, we will focus on the design of a simple fixed-structure robust controller.

To directly focus on the very bulk of this control problem, consider the signal displayed in Fig. 1. This signal represents the rotational speed of the output shaft of the reverser and is proportional to the longitudinal speed of the vehicle. The inversion starts at a forward speed of 1250 rpm (which corresponds to about 10 km/h) and ends, after about 3 s, at a reverse speed of 1250 rpm. The signal shown in Fig. 1 represents the absolute value of the speed. This speed is always positive, since the vehicle is equipped with rotational encoders, which cannot detect the sign of the rotation; the zero crossing obviously indicates the change in the speed direction.

In principle, the “ideal” behaviour of the speed during an inversion is a constant-slope ramp (V-shaped, if we consider the absolute value). Instead, note that the actual measured behaviour displayed in Fig. 1 strongly differs from this ideal pattern: the braking and the accelerating behaviour are asymmetric and the speed is affected by strong oscillations. The result is an uncomfortable inversion.

Starting from the results displayed in Fig. 1 (obtained with a very basic and empirically tuned version of automatic motion inverter control system, which originally equipped the testing prototype used in this work), the objective of this paper is to present and discuss the whole design procedure of a fully automatic inversion system.

The design of this control system can be divided into three subtasks: the design of the inner loop for the control of the EVP current; the design of the open-loop strategies that must be adopted in the first part of the inversion; the design of the main outer loop, which regulates the vehicle speed during

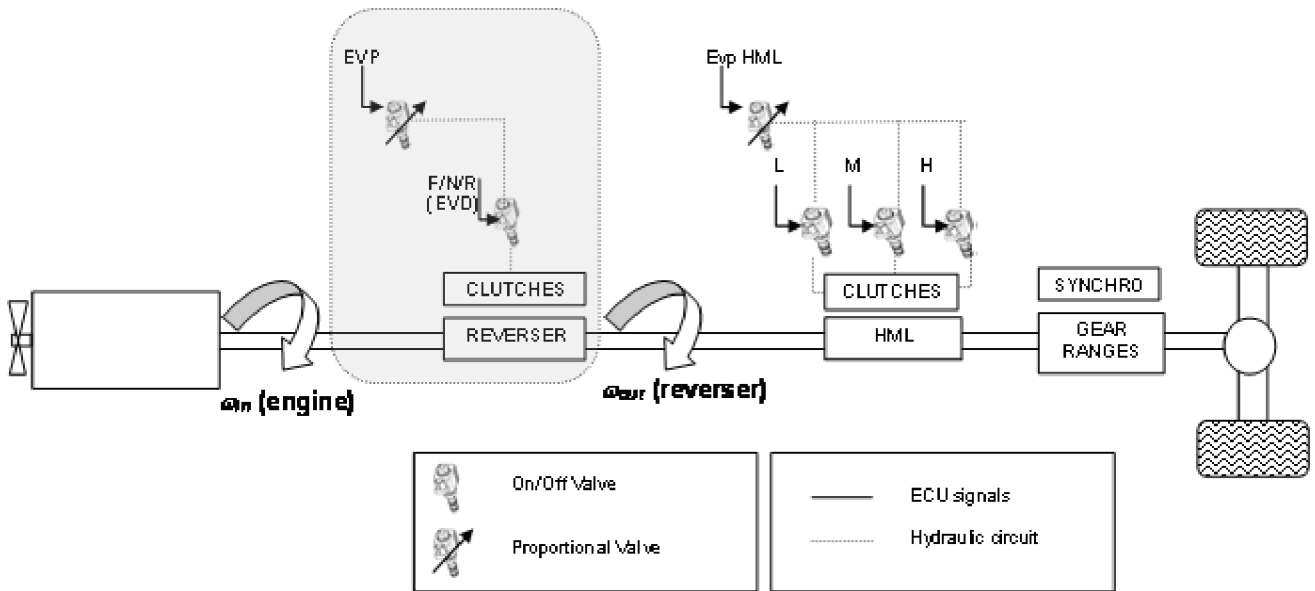


Fig. 2. Structure of the overall power-shuttle transmission system.

the inversion. These three control tasks will be discussed in Sections III–V, respectively. In Section II, a preliminary brief description of the system under control is provided.

The design of a fully automatic motion inverter for agricultural tractors is a comparatively new control problem. The automatic inverter is expected to rapidly become a standard, but only recently designed tractors are equipped with this device. To the best of our knowledge, this control problem has never been treated in the scientific literature, even if many related transmission control systems have been described and proposed (see, e.g., [1]–[3], [6], [7], [9]–[11], [13], [15], [17], [19], [20], [26]–[28], [30], [32], [33], and [36]). In particular, this problem is similar to the more classical automotive clutch-to-clutch automatic transmission shift control problem, since two clutches must be synchronized in speed and torque by electro-hydraulic circuits to achieve a smooth change in output speeds. The automatically shifted manual transmission is also directly analogous because power and speed reversal coordination is a necessary vehicle operation of consideration through no supplemental means but with a single clutch (see, e.g., [2], [12], [16], [31], [34], and [35], where these problems are widely discussed).

The material presented herein is based on a joint project developed on a prototype vehicle (developed for scientific research purposes) by Politecnico di Milano and the R&D Department of the SAME Deutz–Fahr Group. This work has been developed on a modern power-shuttle transmission system designed for low-power tractors. All the data and experimental results described in this work only refer to a prototype transmission group (they do not refer to any SAME Deutz–Fahr vehicle currently in production, which are equipped with a significantly different transmission and control package).

II. SYSTEM DESCRIPTION

The overall scheme of the power-shuttle transmission used in this work is displayed in Fig. 2. Moving from left (engine) to

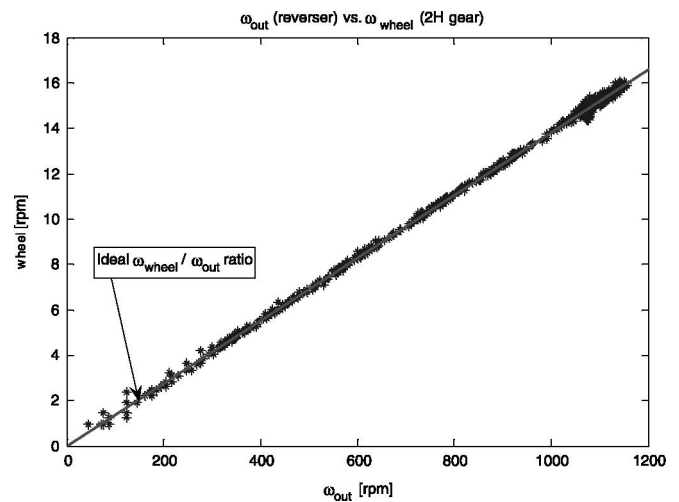


Fig. 3. Relationship (measured and ideal) between wheel speed and output speed ω_{out} (* indicates measured points).

right (wheels), note that the transmission mainly comprises the reverser (shaded box), the three main clutches (low, medium, high), and the synchro. This paper will focus on the reverser only. Accordingly, it will be assumed that the remaining part of the transmission can be simply modeled with a transmission inertia and a fixed transmission ratio.

The main measured variables of the reverser are the input (engine) speed ω_{in} and the output speed ω_{out} . In the rest of the paper, ω_{out} will be assumed to be simply proportional to the wheel speed, according to a transmission ratio. The validity of this assumption is confirmed by the experimental data displayed in Fig. 3.

The reverser is actuated by two electrohydraulic valves: An EVP and an ON-OFF EVD, which is three-way positioned [F (forward), N (neutral), and R (reverse)].

A schematic diagram of the hydraulic circuit, which drives the reverser, is displayed in Fig. 4. Note that it mainly consists

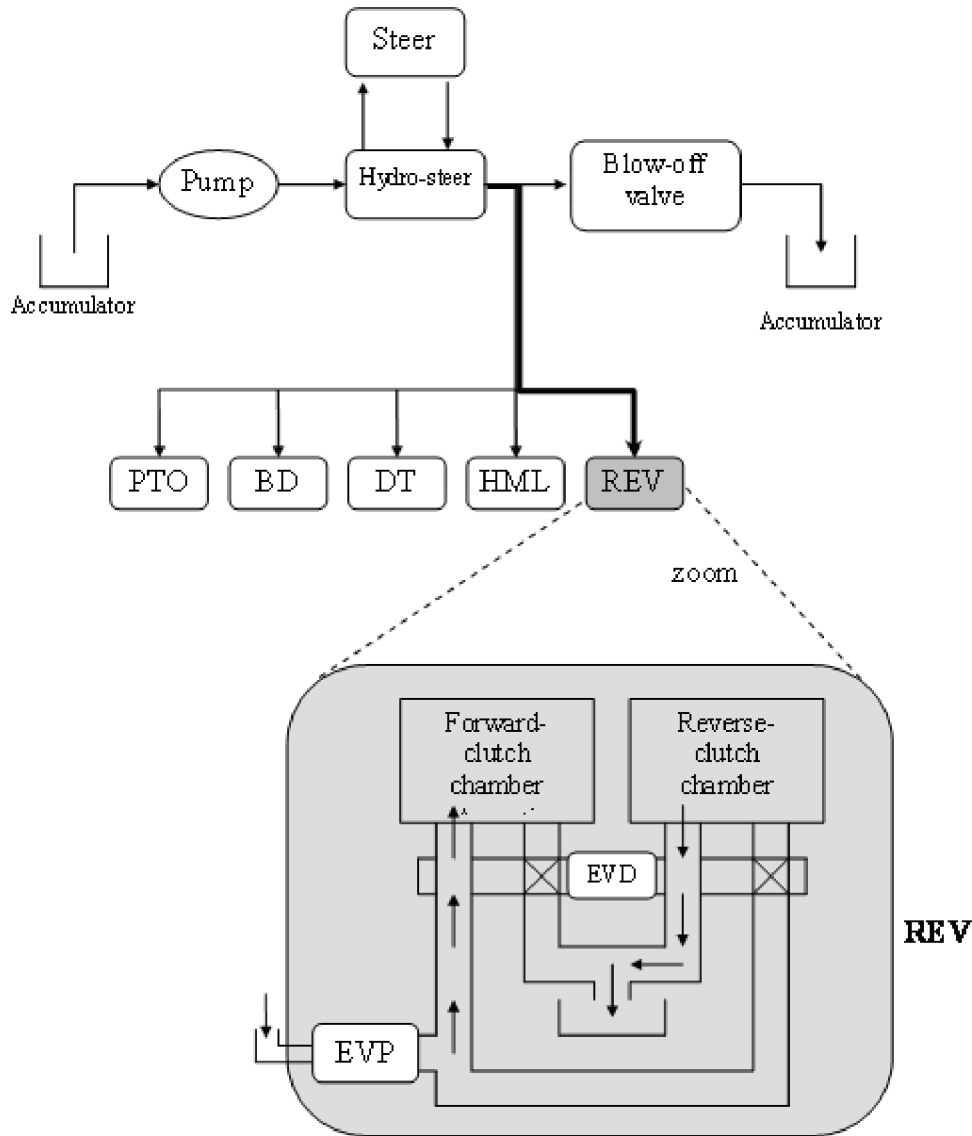


Fig. 4. Hydraulic circuit (in the shaded box the inversion system is zoomed).

of an accumulator, a pump, and many hydraulic “users”: The hydrosteer, the power take off (PTO), the differential-locking system (BD), the all-wheels traction system (DT), the HML clutches, and the reverser (REV).

The reverser (see details in the zoomed part of Fig. 4) is constituted by two clutches (forward and reverse); a clutch is active (namely it transmits some torque) if the hydraulic fluid in the corresponding chamber is pressurized. The bulk of the control problem is to synchronize the activation and the deactivation of these two clutches (this task is done by the EVD), while providing smooth torque transitions (this task is done by the EVP, by continuously modulating the pressure in the clutch chambers).

This control problem will be split into the following three subproblems:

- 1) the control of the current of the EVP (inner loop);
- 2) the open-loop strategy for the EVD and the EVP, during the first part of the inversion (about 0.5 s);

- 3) the closed-loop control of the vehicle speed, using the EVP (outer loop).

These control problems will be discussed in Sections III–V; for each control problem, a solution will be proposed and experimentally validated.

III. INNER LOOP: CLOSED-LOOP CONTROL OF THE EVP CURRENT

The ultimate goal of the EVP in the reverser is to modulate the chamber pressure of the active clutch, whereas the selection of the chamber is done by the EVD. However, the accurate measurement of the output pressure of the EVP in practice is not available due to cost restrictions; the only measured variable of the EVP is the internal current of the valve electro-mechanical driver. The relationship between the EVP current and its output pressure is displayed, in the frequency domain, in Fig. 5. This relationship is purely algebraic (it can be approximated with a

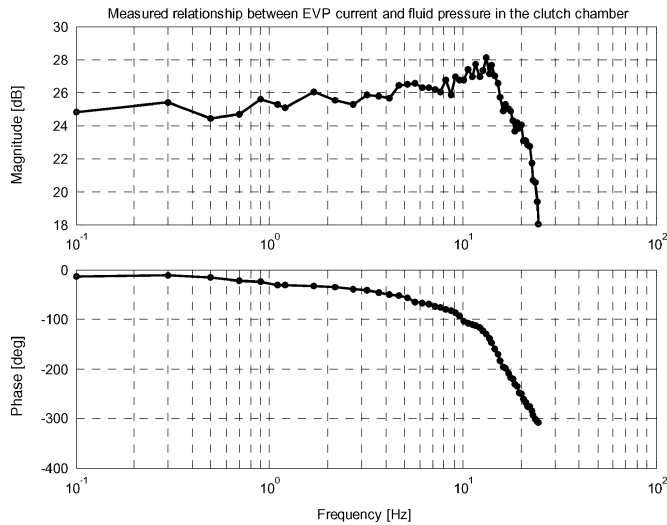


Fig. 5. Relationship between the EVP current and the output pressure in the frequency domain (measured).

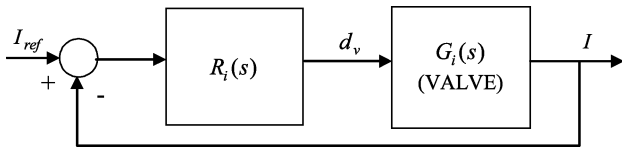


Fig. 6. Control scheme of the inner loop for the control of the EVP current.

simple constant gain) up to about 10 Hz. Within this bandwidth, we can roughly assume that the regulation of the current is equivalent to the regulation of the output pressure. Beyond this frequency, the relationship between these two variables becomes more complex, since it is affected by the dynamics of the clutch chamber.

The main motivation for designing an inner-loop regulator of the EVP is to reduce the nonlinear behaviour of the valve and the effect of the disturbances on the input/output pressures of the EVP. This is the typical rationale of a cascade-control scheme, which consists of a fast inner loop and a slower outer loop [8], [14], [23]. The structure of the inner loop is depicted in Fig. 6; it is a standard single-input-single-output (SISO) control scheme, where the controlled variable is the valve current I , the control input d_v is the pulse-width-modulated (PWM) input signal of the valve, and the reference signal is the desired value of the valve current I_{ref} . $G_i(s)$ is the transfer function that models the I/O dynamics of the valve from d_v to I (linear and time-invariant dynamics are assumed), and $R_i(s)$ is the transfer function of the controller.

To design the current loop, a classical model-based indirect design approach has been used [3], [7]. First, the dynamic behaviour of the plant (from the PWM-modulated input d_v to the output current I of the EVP) has been identified using a frequency-domain identification procedure [18], [29]. By feeding the EVP with multifrequency sinusoidal inputs [4], [5], [18], [21], [22], [24], the frequency response has been experimentally computed. These points have been approximated with a simple linear model consisting of a first-order transfer function and a

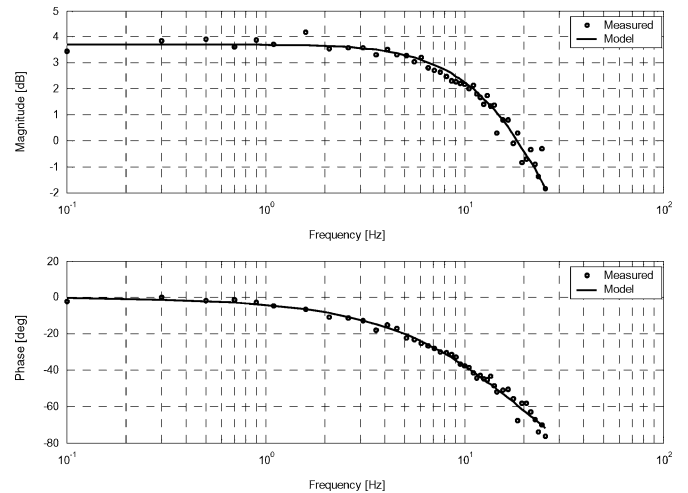


Fig. 7. Experimentally measured (dots) and modeled (continuous line) frequency response of the EVP.

time delay

$$G_i(s) = \frac{K}{1 + sT} e^{-\tau s}.$$

The estimated parameters of this transfer function are $[\hat{K} \ \hat{T} \ \hat{\tau}] = [1.54 \ 10 \ 1.5]$. The fitting between modeled and measured frequency response is very accurate, as shown in Fig. 7.

On the basis of the above model, a simple PI regulator has been designed: $R_i(s) = K_R \frac{1+sT_I}{sT}$, $[K_R \ T_I] = [1 \ 10]$.

The behaviour of the closed-loop system is displayed in Fig. 8, where the measured frequency response of the designed closed-loop system (from the desired current I_{ref} to the measured current I) is displayed. The bandwidth of the closed-loop system is about 26 Hz. This strongly improves the behaviour of the existing empirically tuned controller.

The performance of the control system can be also appreciated in the time domain: in Fig. 9, the measured step responses are displayed. Note that the closed-loop system is faster than the open-loop system (at the price of a little overshoot) and it works much better than the empirically tuned controller.

Since the dynamics of the outer loop are much slower, in the following sections it will be simply assumed that $I \approx I_{ref}$; this approximation obviously is valid only within the bandwidth (0–26 Hz) of the current inner loop.

IV. FIRST 450 MS OF THE INVERSION: OPEN-LOOP STRATEGIES

When the driver requires a motion inversion, the automatic control system takes full control of the vehicle, until its longitudinal speed has reached the same value, with opposite direction. A complete inversion (starting from a maximum speed of 10 km/h) usually takes 3–4 s.

When the automatic inversion procedure starts, the first phase of the inversion algorithm is performed in open loop. According to the open-loop control strategy presented in this section, this phase is 450-ms long [25]. During this open-loop phase the

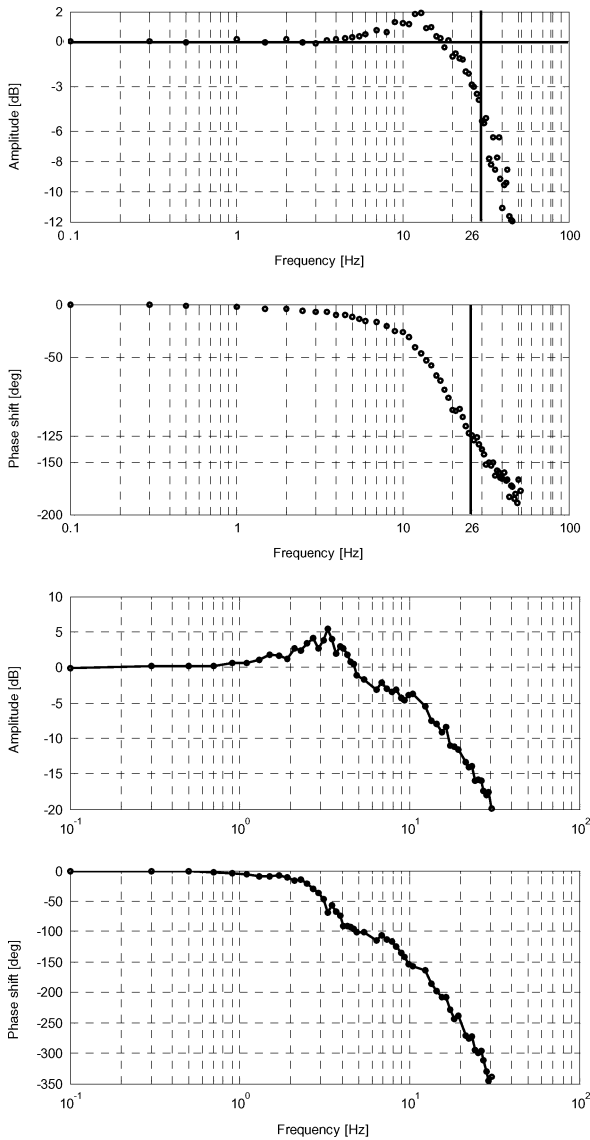


Fig. 8. Frequency-domain behavior of the designed closed-loop system (top) and the empirically tuned controller (bottom).

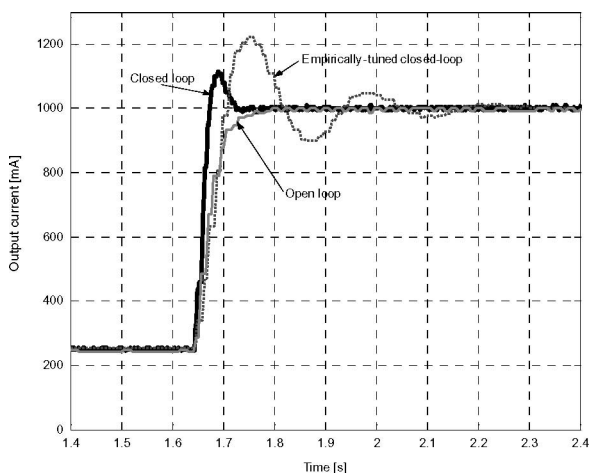


Fig. 9. Step responses of the current of the EVP (measured).

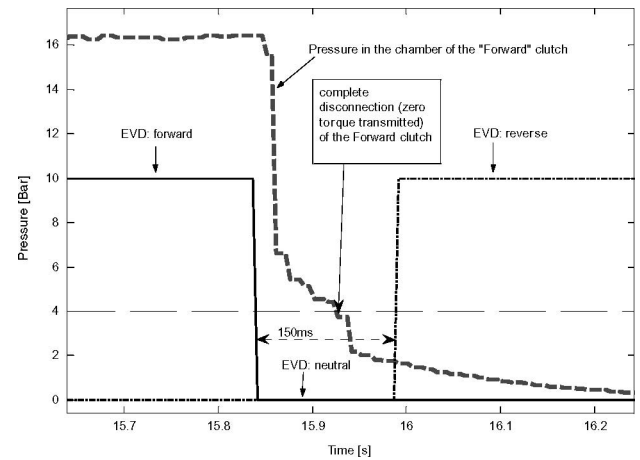


Fig. 10. Switching strategy of EVD.

following actions are taken (consider, for example, an inversion from forward to reverse).

- *EVD*: When the inversion procedure is triggered by the driver, the EVD, which was in the forward position, is immediately switched to the neutral position (see Fig. 10). Since the EVP is closed, the pressure in the chamber of the forward clutch immediately drops; when this pressure goes below (about) four bar, the forward clutch is completely disconnected (no torque is transmitted). When the disconnection of the forward clutch is completed, the EVD switches to the reverse position and the chamber of the reverse clutch starts getting filled. In practice, since clutch pressure is not measured, the EVD is switched from neutral to reverse not immediately after the pressure in the forward chamber drops below 4 bar, but after exactly 150 ms (see Fig. 10). This time window has been empirically estimated in order to guarantee the complete disconnection of the clutch in every working condition.
- *EVP*: When the inversion starts, the EVP is immediately fully closed in order to allow the quickest pressure drop in the forward clutch. When the EVD is switched to the reverse position (after 150 ms), the EVP is reopened in order to allow the rise of the pressure in the reverse clutch chamber. The open-loop design problem is to find the best 300-ms long shape of the EVP current. We will now discuss this problem (and the solution proposed).

We can say that the amount of torque transmitted by the clutch (which is the so called transmission ratio τ) increases from 0% to 100% as the EVP current increases from 0% to 100% (where the 100% condition corresponds, in our EVP, to $I = 1400$ mA). The relationship between the EVP current and the transmission ratio is nondecreasing monotone, but unfortunately it is far from being linear (and, because of the chamber-filling dynamics, it is not even a genuine static function). This relationship $\tau(I) \approx \tau(I_{ref})$ is roughly described in Fig. 11, where the following four current ranges are represented.

- 1) In the lowest current range, the corresponding pressure in the clutch chamber is lower than about 4 bar and no torque is transmitted by the clutch: $\tau(I) = 0, I \in [I_{min}, I_C]$; this current range is a “dead-zone” for the clutch.

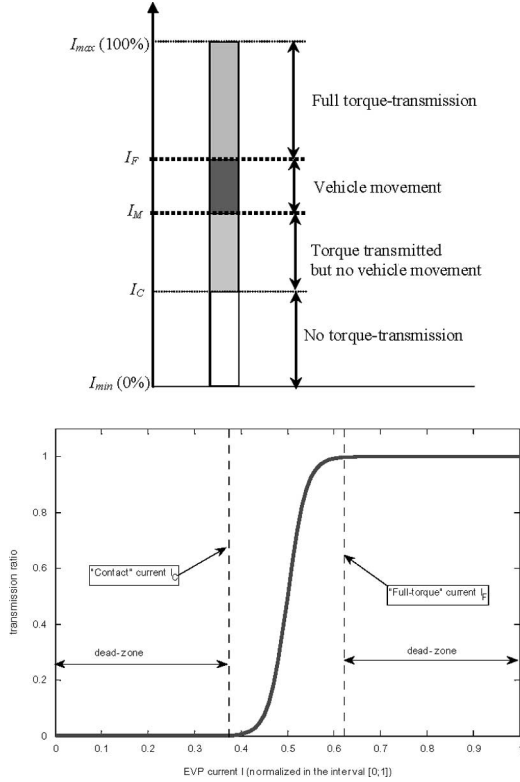


Fig. 11. Qualitative EVP-current ranges (top) and relationship $\tau(I)$ (bottom).

- 2) In the second current range ($I \in [I_C, I_M]$), some torque is transmitted by the clutch, but this torque is lower than the overall static friction torques acting on the vehicle (if the vehicle starts from a still condition). Here, the current I_C is called “Contact” current (since the clutch begins to establish a contact between its input and output shafts) and the current I_M is called “movement” current (since the clutch starts to move the vehicle).
- 3) In the third current range (from $I \in [I_M, I_F]$), the transmitted torque increases from the minimum “Movement” level to 100% (the current I_F is called “Full” transmission current).
- 4) The last current range corresponds to full-torque transmission: $\tau(I) = 1, I \in [I_F, I_{max}]$; this current range is also a “dead-zone” from the control-designer point of view.

The problem is how to bring the EVP current from $I_{min} = 0$ to I_M in 300 ms. From Fig. 12, it is apparent that this task is made difficult by the narrow modulation range of the current, since the curve $\tau(I)$ is very skewed. However, the major problem is that the value I_M is spread over a large range. As a matter of fact, unfortunately, the value of I_M can be strongly affected by:

- differences between different vehicles, due to construction tolerances;
- different working temperatures;
- different loads and masses of the vehicle;
- different slopes of the road where the vehicle is operating;
- different gear ratios.

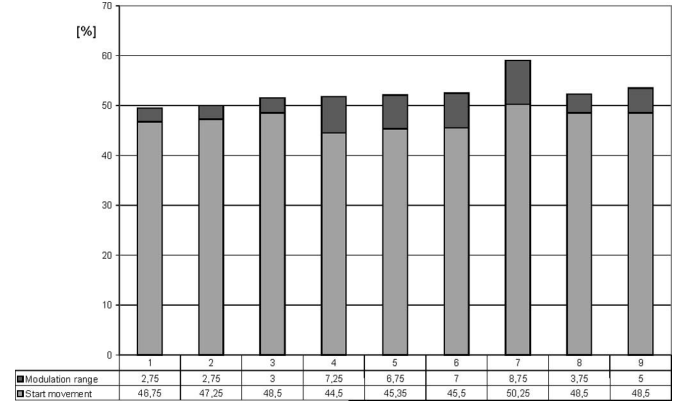


Fig. 12. $[I_{min}, I_M]$ and $[I_M, I_F]$ EVP-current ranges measured in nine different working conditions.

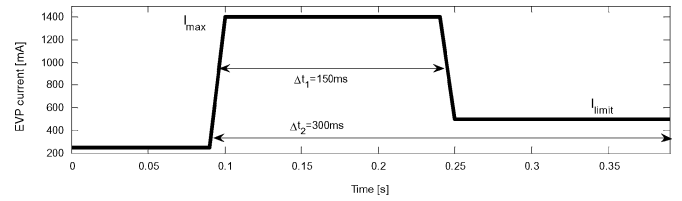


Fig. 13. Shape of the EVP current, during the open-loop phase, proposed in this work.

To better understand this issue, in Fig. 12, the results of an experimental procedure aimed to identify I_M and I_F are displayed; the same vehicle has been used, but nine different working conditions (different temperatures, loads, and gear ratios) have been tested. In this figure, the experimentally measured current range $[I_M, I_F]$ is displayed. The results in Fig. 12 are very interesting but, somehow, discouraging. Note that:

- the values of I_M range from a minimum of 44.5% to a maximum of 50.25% (spread of about 6%);
- the modulation range $I_F - I_M$ ranges from a minimum of 2.75% (!) to a maximum of 8.75%.

These results show that the modulation range is very small, if compared with the spread of I_M . This makes the overall control problem very challenging. Since the value of I_M can vary and cannot be estimated online, the following two undesired situations may occur.

- 1) The actual value of I_M is lower than the nominal value of I_M : in this case, the open-loop procedure brings the EVP current to a value higher than the “Movement” current. This would cause discomfort since it results in a step in the transmitted torque (the reverse clutch is over activated).
- 2) The actual value of I_M is higher than the nominal value of I_M : In this case, the open-loop procedure brings the EVP current to a value lower than the “Movement” current. This would cause a delay in the activation of the reverse torque, since, when the closed-loop control is activated, the current is not yet positioned at the movement condition (the reverse clutch is under activated).

An acceptable compromise between these conditions must be found. The open-loop EVP-current shape proposed herein is displayed in Fig. 13.

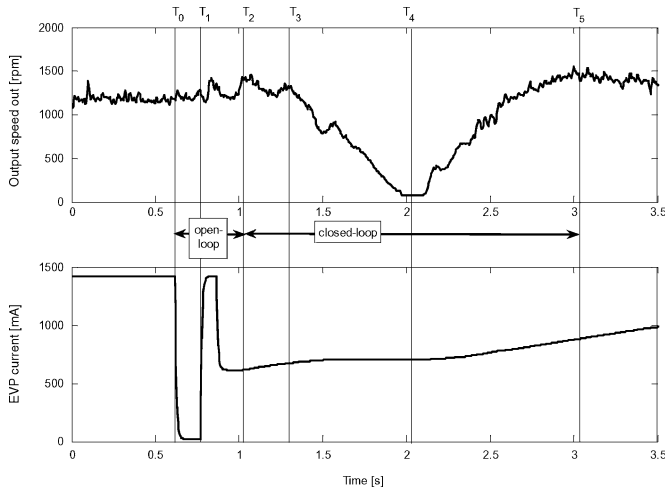


Fig. 14. EVP current and output reverser speed during an inversion procedure.

- When the EVD is switched into the reverse condition (150 ms after the inversion is triggered), the EVD current is switched to I_{max} and it is kept at this value for 150 ms. Even if the EVD current is much higher than I_M in this time window, the actual transmitted torque is slower than the Movement torque. This is due to the fact that the clutch chamber must be filled (when the reverse clutch is activated, its pressure is very low and it is partially empty). This strategy minimizes the filling delay. The time window of 150 ms has been computed in order to guarantee that the movement torque is not reached in every working condition.
- After 150 ms the EVP current is switched from I_{max} to I_{lim} , where I_{lim} is the lowest value of I_M , measured in different working conditions (e.g., $I_{lim} = 44.5\%$, considering the results displayed in Fig. 12). This value of the EVP current is then kept for 150 ms and the closed-loop algorithm is then activated. This strategy guarantees that no torque overshoot occurs at the price of a possible delay in the activation of the movement torque. However, thanks to the previous 150 ms of “full-current” strategy, the overall open-loop phase remains very short and a possible small lag in the reverse torque activation can be accepted.

Note that there are three design parameters for this strategy: The final current I_{lim} , the full-current time window Δt_1 , and the overall time window Δt_2 ; however, since conservative values for both I_{lim} and Δt_1 are used, in practice no vehicle-specific tuning procedure is required. A value of $\Delta t_2 = 300$ ms has been chosen for an overall open-loop time of 0.45 s.

To summarize and to better understand the behaviour of the whole 450 ms of open-loop control, in Fig. 14 the behaviour of the EVP current and the output speed ω_{out} during a complete inversion are displayed. Now observe the following.

- The inversion starts at T_0 : In the interval $T_0 \leftrightarrow T_1$ (150 ms), the EVD is the neutral position and the EVP current is switched to zero in order to accelerate the pressure drop in the forward clutch.
- The interval $T_1 \leftrightarrow T_2$ (300 ms) corresponds to the open-loop control of the EVP. The EVP current is at I_{max} for 150

ms and then it is switched to I_{lim} . During the first 450 ms (open-loop interval $T_0 \leftrightarrow T_2$) of the inversion, the output speed remains almost constant. As a matter of fact, in this time window the transmitted torque is negligible and the vehicle simply keeps its forward speed (thanks to its huge inertia).

- At T_2 , the closed-loop controller on the vehicle speed (which will be extensively described in Section V) is activated. In the time interval $T_2 \leftrightarrow T_3$ (about 200 ms), no speed variation occurs. This can be easily interpreted: due to the conservative choice of I_{lim} , at T_2 , the EVP current can be still lower than the actual value of I_M for that specific working condition; therefore, the closed-loop controller must fill this residual gap before the speed could actually start decreasing.
- In the interval $T_3 \leftrightarrow T_5$, the motion inversion is performed. The sign change of the vehicle speed occurs at T_4 . During $T_3 \leftrightarrow T_5$, the EVP current is modulated by the closed-loop controller within the “modulation range” $I_M \leftrightarrow I_F$. Note that, in practice, after T_4 the EVP current is beyond I_F (the reverse clutch is fully connected).

As already remarked, since the choice of I_{lim} is conservative, at the end of the open-loop procedure the transmitted torque is usually smaller than the movement torque. This open-loop approach hence requires a good (fast and reliable) closed-loop speed control, which can smoothly compensate the open-loop error. This issue will be discussed in Section V.

V. OUTER LOOP: CLOSED-LOOP CONTROL OF THE VEHICLE MOTION

The third control subproblem is most crucial, since it takes care of the ultimate goal of the inversion: the control of the vehicle movement during the inversion. As discussed in Section IV, this outer-loop controller is activated when the open-loop control of the EVP current is concluded. In the open-loop strategy proposed in this work, this happens exactly 450 ms after the inversion is triggered by the driver.

To design the outer loop, the basic dynamics of the regulated system must be modeled. The main dynamics are considered here. It is important to point out that the clutch dynamics are affected by nontrivial nonlinear phenomena (dead zones, hysteretic effects, etc.), which should be included in an accurate simulator of the system. For the outer-loop design purposes, these phenomena can be neglected, at least in the first control-design iteration procedure.

If we consider the longitudinal dynamics of the vehicle, the following second-order model can be written (see, e.g., [34], [35])

$$\begin{cases} J_E \dot{\omega}_{in} = T_E(\omega_{in}; \Phi) - T_C(\omega_{in} - \omega_{out}) - \tau T_L(\omega_{out}) \\ J_V \dot{\omega}_{out} = \tau T_E(\omega_{in}; \Phi) + \tau T_C(\omega_{in} - \omega_{out}) - T_L(\omega_{out}) \end{cases} \quad (1)$$

The variables and functions used in (1) have the following meaning.

- ω_{in} and ω_{out} are the input and output rotational speeds of the reverser and are the state variables of (1).

- J_E is the inertia of the engine.
- J_V is the overall inertia of the vehicle. It includes the rotating parts of the transmission, additional loads, and additional trailers, depends on the current gear transmission, and is subject to large variations.
- $T_E(\omega_{in}; \Phi)$ is the engine torque. It depends on the speed engine ω_{in} and the throttle position Φ .
- $T_L(\omega_{out})$ is the load torque. It is mainly due to friction effects (rolling resistance, aerodynamics forces, etc.) and is proportional to ω_{out}^2 : $T_L(\omega_{out}) \propto \omega_{out}^2$. This load torque may include the effect of a road slope.
- $T_C(\omega_{in} - \omega_{out})$ is the clutch torque. It is a static function of the clutch slip $\omega_{in} - \omega_{out}$. When the clutch is fully connected, this term vanishes: $T_C(0) = 0$. Since T_C is mainly due to friction, it is proportional to $(\omega_{in} - \omega_{out})^2$.
- $\tau \in [0, 1]$ is the transmission ratio. It is the fraction of the torque that the clutch can transmit (note that this transmission ratio applies to both sides of the clutch). It is the control variable of the system and depends on the EVP current: $\tau = \tau(I)$ (we assume that the inner loop is much faster than this outer loop; therefore, we can assume $I = I_{ref}$, see Section III). As already discussed (see Fig. 11), unfortunately the function $\tau(I)$ is far from being a simple linear function of I and the modulation range of the current is very small; we assume that the closed-loop controller works within this narrow modulation range.

Since (1) is a nonlinear model, it is useful to linearize it around an equilibrium condition, namely

$$\begin{cases} 0 = T_E(\bar{\omega}_{in}; \bar{\Phi}) - T_C(\bar{\omega}_{in} - \bar{\omega}_{out}) - \bar{\tau}T_L(\bar{\omega}_{out}) \\ 0 = \bar{\tau}T_E(\bar{\omega}_{in}; \bar{\Phi}) + \bar{\tau}T_C(\bar{\omega}_{in} - \bar{\omega}_{out}) - \bar{T}_L(\bar{\omega}_{out}) \end{cases} \quad (2)$$

Given a transmission ratio $\bar{\tau}$ and a throttle position $\bar{\Phi}$, from (2) the corresponding equilibrium values of $\bar{\omega}_{in}$ and $\bar{\omega}_{out}$ can be found. Around this equilibrium (which is fully defined by $\bar{\tau}$, $\bar{\Phi}$, $\bar{\omega}_{in}$, and $\bar{\omega}_{out}$), the model (1) can be linearized as

$$\begin{cases} J_E \delta \dot{\omega}_{in} = \bar{T}'_E \delta \omega_{in} + \bar{K}_\Phi \delta \Phi - \bar{T}'_C \delta \omega_{in} + \bar{T}'_L \delta \omega_{out} \\ \quad - \bar{\tau} \bar{T}'_L \delta \omega_{out} - \bar{T}_L \delta \tau \\ J_V \delta \dot{\omega}_{out} = \bar{\tau} \bar{T}'_E \delta \omega_{in} + \bar{\tau} \bar{K}_\Phi \delta \Phi + \bar{T}_E \delta \tau + \bar{\tau} \bar{T}'_C \delta \omega_{in} \\ \quad - \bar{\tau} \bar{T}'_C \delta \omega_{out} + \bar{T}_C \delta \tau - \bar{T}'_L \delta \omega_{out} \end{cases}$$

where

$$\begin{aligned} \delta \omega_{out} &= \omega_{out} - \bar{\omega}_{out}, \quad \delta \tau = \tau - \bar{\tau}, \quad \delta \Phi = \Phi - \bar{\Phi}, \\ \bar{T}'_E &= \left. \frac{\partial T_E(x; \bar{\Phi})}{\partial x} \right|_{x=\bar{\omega}_{in}}, \quad \bar{T}'_C = \left. \frac{\partial T_C(x)}{\partial x} \right|_{x=\bar{\omega}_{in} - \bar{\omega}_{out}}, \\ \bar{T}'_L &= \left. \frac{\partial T_L(x)}{\partial x} \right|_{x=\bar{\omega}_{out}}, \quad \bar{K}_\Phi = \left. \frac{\partial T_E(\bar{\omega}_{in}; x)}{\partial x} \right|_{x=\bar{\Phi}}, \\ \bar{T}_E &= T_E(\bar{\omega}_{in}; \bar{\Phi}), \quad \bar{T}_C = T_C(\bar{\omega}_{in} - \bar{\omega}_{out}), \quad \text{and} \\ \bar{T}_L &= T_L(\bar{\omega}_{out}). \end{aligned}$$

To further simplify this model, assume that $\bar{\tau} \gg (1 - \bar{\tau})$ (namely the reverser works around a high transmission ratio). Under this assumption, $(\omega_{in} - \omega_{out})$ is small. Since $T_C(\omega_{in} - \omega_{out}) \propto (\omega_{in} - \omega_{out})^2$, \bar{T}'_C and \bar{T}_C are small and can

be neglected, and therefore we have

$$\begin{cases} J_E \delta \dot{\omega}_{in} \approx \bar{T}'_E \delta \omega_{in} + \bar{K}_\Phi \delta \Phi - \bar{\tau} \bar{T}'_L \delta \omega_{out} - \bar{T}_L \delta \tau \\ J_V \delta \dot{\omega}_{out} \approx \bar{\tau} \bar{T}'_E \delta \omega_{in} + \bar{\tau} \bar{K}_\Phi \delta \Phi + \bar{T}_E \delta \tau - \bar{T}'_L \delta \omega_{out} \end{cases} \quad (3)$$

The engine dynamics and the vehicle dynamics are strongly frequency decoupled, since $J_V \gg J_E$ (the overall vehicle inertia is much larger than the engine inertia). As a consequence, from the vehicles-dynamics point of view, the first equation of (3) can be viewed as a simple algebraic relationship, namely

$$\begin{cases} 0 \approx \bar{T}'_E \delta \omega_{in} + \bar{K}_\Phi \delta \Phi - \bar{\tau} \bar{T}'_L \delta \omega_{out} - \bar{T}_L \delta \tau \\ J_V \delta \dot{\omega}_{out} \approx \bar{\tau} \bar{T}'_E \delta \omega_{in} + \bar{\tau} \bar{K}_\Phi \delta \Phi + \bar{T}_E \delta \tau - \bar{T}'_L \delta \omega_{out} \end{cases} \\ \Rightarrow \begin{cases} \delta \omega_{in} \approx -\frac{\bar{K}_\Phi}{\bar{T}'_E} \delta \Phi + \frac{\bar{\tau} \bar{T}'_L}{\bar{T}'_E} \delta \omega_{out} + \frac{\bar{T}_L}{\bar{T}'_E} \delta \tau \\ J_V \delta \dot{\omega}_{out} \approx \bar{\tau} \bar{T}'_E \delta \omega_{in} + \bar{\tau} \bar{K}_\Phi \delta \Phi + \bar{T}_E \delta \tau - \bar{T}'_L \delta \omega_{out} \end{cases} \quad (4)$$

By plugging the expression $\delta \omega_{in}$ into the second equation of (4), the following first-order linear dynamic equation is obtained (the effect of a throttle disturbance on the output speed is negligible)

$$\delta \dot{\omega}_{out} \approx -\frac{1}{J_V} [(1 - \bar{\tau}^2) \bar{T}'_L] \delta \omega_{out} + \frac{1}{J_V} [\bar{T}_E + \bar{\tau} \bar{T}'_L] \delta \tau.$$

The relationship between the input $\delta \tau$ and the output $\delta \omega_{out}$ can hence be described by

$$G(s) = \frac{\frac{1}{J_V} [\bar{T}_E + \bar{\tau} \bar{T}'_L]}{s + \frac{1}{J_V} [(1 - \bar{\tau}^2) \bar{T}'_L]}. \quad (5)$$

Consider now the ratio ω_{out}/ω_{in} . Since the actual value of τ can hardly be measured, ω_{out}/ω_{in} is usually considered a good approximation of the transmission ratio. Around a working condition, it can be written as

$$\delta \left(\frac{\omega_{out}}{\omega_{in}} \right) = \left[\frac{1}{\bar{\omega}_{in}} \right] \delta \omega_{out} + \left[-\frac{\bar{\omega}_{out}}{\bar{\omega}_{in}^2} \right] \delta \omega_{in}. \quad (6)$$

By plugging the expression (4) of $\delta \omega_{in}$ in (6), this can be rewritten as

$$\begin{aligned} \delta \left(\frac{\omega_{out}}{\omega_{in}} \right) &= \left[\frac{1}{\bar{\omega}_{in}} - \frac{\bar{\omega}_{out}}{\bar{\omega}_{in}^2} \frac{\bar{\tau} \bar{T}'_L}{\bar{T}'_E} \right] \delta \omega_{out} + \left[-\frac{\bar{\omega}_{out}}{\bar{\omega}_{in}^2} \frac{\bar{T}_L}{\bar{T}'_E} \right] \delta \tau \\ &\quad + \left[\frac{\bar{\omega}_{out}}{\bar{\omega}_{in}^2} \frac{\bar{K}_\Phi}{\bar{T}'_E} \right] \delta \Phi. \end{aligned} \quad (7)$$

The block diagram of the approximate linearized model (5)–(7) is depicted in Fig. 15. Observe that the system is characterized by a control input given by the I -driven transmission ratio ($\delta \tau$), a disturbance given by the throttle position ($\delta \Phi$). Three controlled outputs can be considered: The ratio $\delta(\omega_{out}/\omega_{in})$, the output speed $\delta \omega_{out}$ (which is proportional to the longitudinal speed of the vehicle), and the output acceleration $\delta \dot{\omega}_{out}$ (which is proportional to the longitudinal acceleration of the vehicle). Since a single control input is available, it is natural to design a SISO control loop. A key issue therefore is the selection of a wise output (controlled) variable. A concise

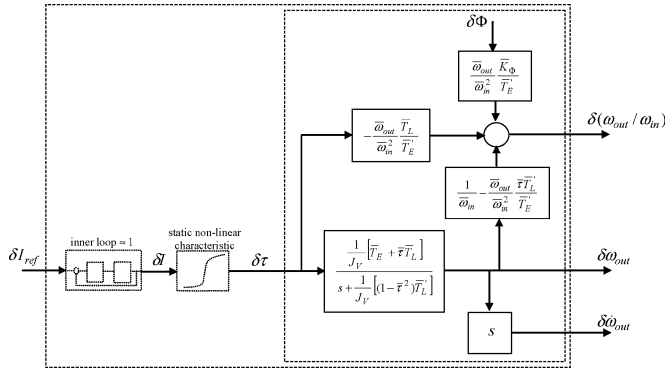


Fig. 15. Block diagram of the approximate linear model.

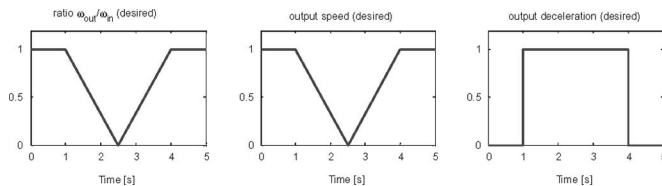


Fig. 16. Normalized absolute values of the reference signals for the three candidate output controlled variables.

discussion on each of the above three candidate outputs is now provided.

The output speed ω_{out} is a natural and intuitive controlled variable. As a matter of fact, the inversion procedure can be seen as the smooth transition between $\omega_{out} = 1$ and $\omega_{out} = -1$ (these values are normalized with respect to the initial speed). Accordingly, the reference-trajectory for $|\omega_{out}|$ during a 3-s long inversion (see Fig. 16) is a V-shaped function. From the dynamical point of view, the control of this variable is not particularly critical. The transfer function from $\delta\tau$ to $\delta\omega_{out}$ is a simple first-order system given by (5) and $\delta\omega_{out}$ is almost not affected by throttle disturbances. The major flaw of the choice of ω_{out} , however, is that it is difficult to synchronize the V-shaped reference signal during the inversion procedure. In the previous section it has been shown that, due to the uncertainties to the “motion” current I_M , it is difficult to exactly predict when the vehicle speed actually will start decreasing. Since the control of ω_{out} is a reference-tracking control problem, which must be precisely time synchronized, a fixed V-shaped reference signal starting at the end of the open-loop phase may result in undesired bumps and oscillations in the vehicle speed.

The ratio $(\omega_{out}/\omega_{in})$ is another natural controlled variable since it is a good approximation of the transmission ratio. Similar to ω_{out} , the reference trajectory for $|\omega_{out}/\omega_{in}|$ during a 3-s long inversion is V-shaped, the control of this variable is not dynamically critical, but it is difficult to synchronize the V-shaped reference signal.

Under the assumption that, during the inversion, the input engine speed ω_{in} is constant, it may be noted that the regulation of $(\omega_{out}/\omega_{in})$ is equivalent to the regulation of ω_{out} . However, in practice, during an inversion the engine speed is subject to large

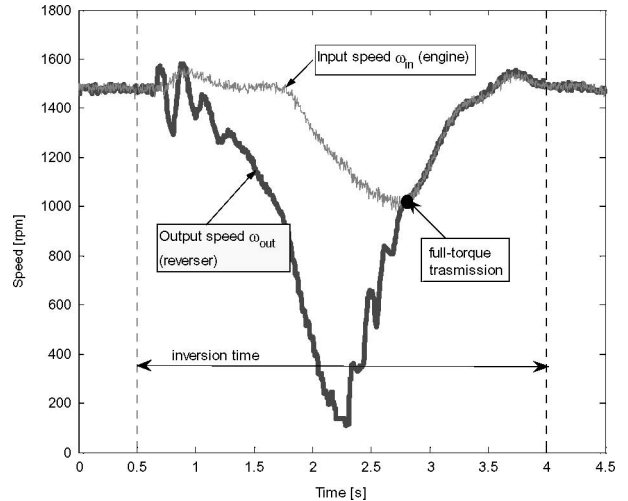


Fig. 17. Input and output speeds of the reverser during an inversion.

variations, which can be clearly seen in Fig. 17. The major consequence is that the control of a constant slope $(\omega_{out}/\omega_{in})$ does not guarantee a constant-deceleration behaviour of the vehicle. Using $(\omega_{out}/\omega_{in})$ as a controlled variable produces a large distortion in the behaviour of the vehicle speed; hence, $(\omega_{out}/\omega_{in})$ is a poor choice as a controlled variable.

The output acceleration $\dot{\omega}_{out}$ does not suffer of the flaws affecting ω_{out} and $(\omega_{out}/\omega_{in})$: The controller can be designed as a simple regulation loop (with constant set point). Accordingly, no synchronization problems of the reference trajectory arise. Moreover, the behaviour of $\dot{\omega}_{out}$ is not distorted by variations of the engine speed during the inversion. The output acceleration $\dot{\omega}_{out}$ hence is the best controlled variable.

We conclude this section by presenting the results obtained with the closed-loop control of the acceleration (a standard PI controller has been used). They are compared with the results obtained with a closed-loop controller on $(\omega_{out}/\omega_{in})$, which originally equipped the prototype vehicle we used.

In Fig. 18, the inversions for a vehicle in four different working conditions are displayed: A vehicle in standard configuration, a vehicle with an additional load of 1000 kg, a vehicle with an additional trailer of 5000 kg, and a vehicle in standard configuration traveling on an uphill road. The control strategy used in these three cases is the same (no adaptations with respect to the vehicle conditions are made). Also, all the other working conditions are the same (initial and final speed, gear ratio, etc.). Note that the tested mass variations are remarkably large, since the vehicle, in its standard configuration, has a mass of about 2500 kg.

From Fig. 19, the advantage of using the output acceleration as control variable is obvious. Note that the deceleration and acceleration phases are very similar and symmetric, bumps and oscillations on the vehicle speed are much lower, and the overall inversion is consistently performed in a slightly shorter time. Most importantly, the behaviour of the closed-loop system shows little sensitivity to changes in the vehicle conditions. Similar results have been obtained in different gear ratios and at different working temperatures. The overall results are very

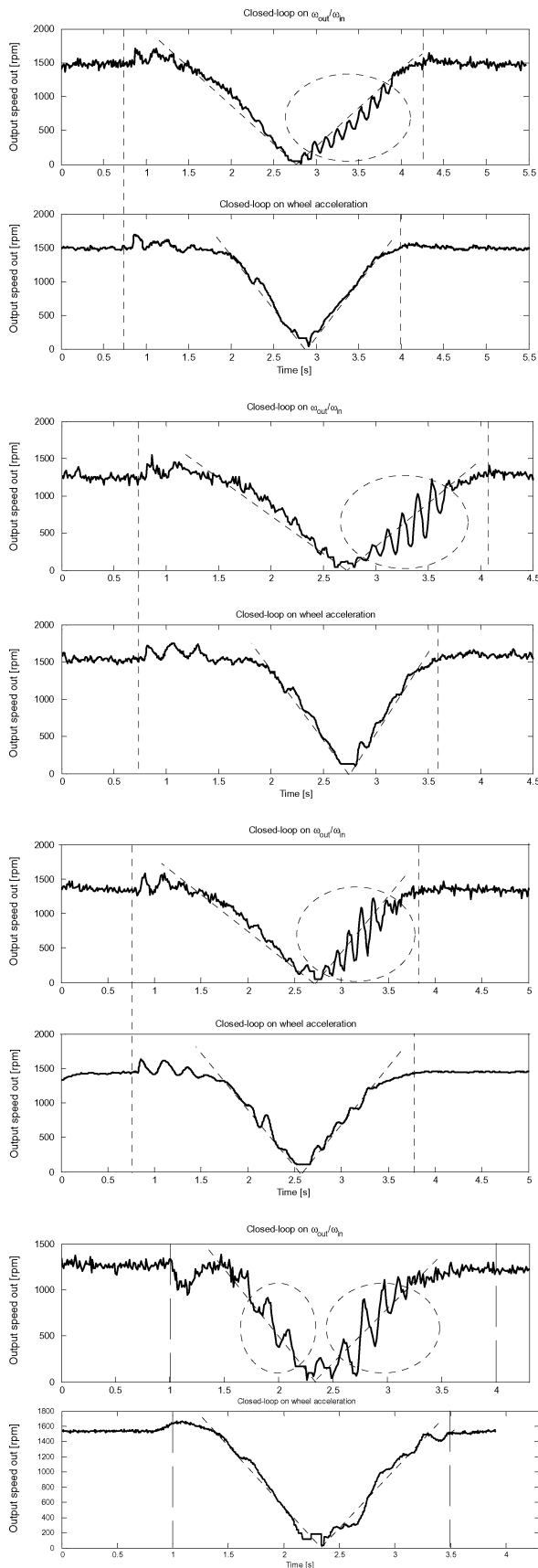


Fig. 18. Inversion of the vehicle in four conditions. From top to bottom: standard configuration; additional load of 1000 kg; additional trailer of 5000 kg; standard configuration, uphill.

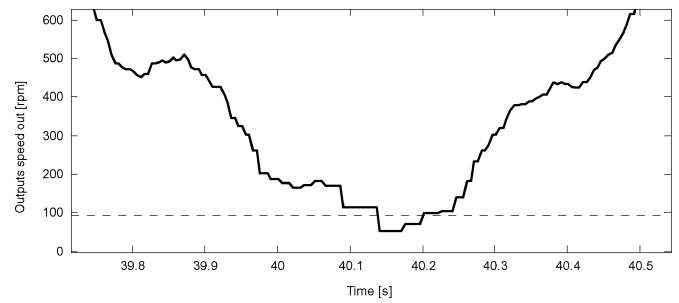


Fig. 19. Detail of the measured rotation speed at the output of the reverser during a zero-speed crossing.

satisfactory. The system requires little tuning and consistently provides good results over a wide range of working conditions.

Remark (supervisory control unit): It is important to observe that, in principle, if an external force prevents the vehicle from moving in the reversed direction, then the vehicle output cannot follow the desired profiles shown in Fig. 17, and the outer loop (the closed-loop vehicle motion control) may cause engine stall. This happens in all the above-mentioned controller schemes. This issue has not been specifically treated in the prototype control scheme presented in this work. However, a complete version of the control architecture should be equipped with a supervisory unit (typically implemented as a finite state machine), which takes care of exceptional events, fault detection and management, parameter adaptations, etc.

Remark (throttle perturbations): All the experiments are essentially performed in fixed-throttle conditions. However, it is useful to remark that the engine is equipped with a slow feedback rpm regulator, which is active during the inversion experiments presented herein. Thanks to the low bandwidth of this regulation loop, in practice, the dynamic interaction with the outer loop of the motion inverter is negligible and the throttle variations induced by the rpm regulator can be simply treated as external disturbances.

Remark (speed measurement): A well-known problem in the regulation of a rotational speed (or of variables that can be indirectly computed from a rotational speed) is the accurate measurement of the speed at low rpm, if it is measured with a standard Hall-effect encoder. As a matter of fact, since the rotation speed is measured from the time elapsed between two consecutive pulses, when the speed approaches zero, the quantization error rapidly grows. This issue has been discussed in detail, e.g., in [20]. This problem is clearly visible in Fig. 19, where the measured rotation speed of the reverser output is displayed around a zero crossing. The measurement device used in the test prototype is a standard low-cost 24-steps encoder; it is clear that the quantization error becomes unacceptable below (about) 100 rpm. This problem inherently affects the measurement technology and can be fully solved only with an analog measurement device, or it can be attenuated (in principle, at any desired level of accuracy) by increasing the number of steps of the encoder (the tradeoff obviously being the sensor cost).

With respect to this issue, it is interesting to remark that, in the control architecture presented in this work, this problem has been simply solved by “freezing” the controller state vector

in the short time window (typically 200–300 ms) when the measured speed is in the range $[-100, +100]$ rpm. The effect of this simple modification on the main control loop is negligible and the potential improvements achievable using a finer encoder does not balance the additional sensor cost.

VI. CONCLUDING REMARKS

In this paper, the three main control tasks (EVP-current control, EVD–EVP open-loop modulation, and closed-loop control of the vehicle longitudinal motion) of an automatic motion inverter are analyzed and a complete control solution is proposed and experimentally tested.

The final results are very satisfactory and consistently provide a comfortable inversion over a wide range of working conditions, using a simple fixed-structure controller, which requires little or no tuning.

Some intrinsic limitations of the system are also outlined. In particular, a flatter characteristic between the EVP current and the transmission ratio could further improve the comfort of the inversion, without changing the main rationale of the algorithms proposed herein.

ACKNOWLEDGMENT

The authors would like to thank A. Mangili for his help in the implementation and analysis of the identification and control algorithms presented in this work.

REFERENCES

- [1] J. V. Amerongen, "Mechatronic design," *J. Mechatronics*, vol. 13, no. 10, pp. 1045–1066, 2003.
- [2] S. Bai, R. Moses, T. Schanz, and M. J. Gorman, "Development of a new clutch-to-clutch shift control technology," presented at the SAE 2002 World Congr. & Exhibition, Detroit, MI, Mar. 2002, Paper SAE 2002-01-1252.
- [3] M. B. Barron and W. F. Powers, "The role of electronic controls for future automotive mechatronic systems," *IEEE/ASME Trans. Mechatronics*, vol. 1, no. 1, pp. 80–88, Mar. 1996.
- [4] S. Bittanti and G. Picci, Eds., *Identification, Adaptation, Learning—The Science of Learning Models from Data*, Computer and Systems Sciences Series. Berlin, Germany: Springer-Verlag, 1996.
- [5] S. Bittanti and S. M. Savaresi, "On the parametrization and design of an extended kalman filter frequency tracker," *IEEE Trans. Autom. Control*, vol. 45, no. 9, pp. 1718–1724, Sep. 2000.
- [6] Y. Cheng and B. L. R. De Moor, "Robustness analysis and control system design for a hydraulic servo system," *IEEE Trans. Control Syst. Technol.*, vol. 2, no. 3, pp. 183–197, Sep. 1994.
- [7] L. Glielmo and F. Vasca, "Engagement control for automotive dry clutch," in *Amer. Control Conf.*, 2000, vol. 2, pp. 1016–1017.
- [8] G. O. Guardabassi and S. M. Savaresi, "Approximate linearization via feedback—An overview," Survey paper, *Automatica*, vol. 27, pp. 1–15, 2001.
- [9] L. Guzzella and C. H. Onder, *Introduction to Modeling and Control of Internal Combustion Engines*. Berlin, Germany: Springer-Verlag, 2004.
- [10] R. Isermann, *Mechatronic Systems—Fundamentals*. London: Springer-Verlag, 2003.
- [11] U. Kiencke and L. Nielsen, *Automotive Control Systems for Engine, Driveline, and Vehicle*. Berlin, Germany: Springer-Verlag, 2000.
- [12] M. Leising, H. Benford, and G. Holbrook, "The all-adaptive controls for the chrysler ultradrive transaxle," SAE paper 890529, 1989.
- [13] S. Liu and B. Paden, "A survey of today's CVT controls," in *36th IEEE Decision Control Conf.*, 1997, vol. 5, pp. 4738–4743.
- [14] C. L. Ren and C. Long-Yeu, "Stabilization for linear uncertain system with time latency," *IEEE Trans. Ind. Electron.*, vol. 49, no. 4, pp. 905–910, Aug. 2002.
- [15] G. Mantriota, "Theoretical and experimental study of a power split continuously variable transmission system Part 1," *J. Automobile Eng.*, vol. 215, no. 7, pp. 837–850, 2001.
- [16] T. Megli, M. Haghgooe, and D. S. Colvin, "Shift characteristics of a 4-speed automatic transmission," presented at the Int. Congr. Expo, Detroit, MI, Mar. 1999, Paper SAE 1999-01-1060.
- [17] K. Nevala, J. Penttinen, and P. Saavalainen, "Developing of the anti-slip control of hydrostatic power transmission for forest tractor and optimization of the power of diesel engine," in *5th Int. Workshop Adv. Motion Control*, 1998, pp. 475–480.
- [18] R. Pintelon and J. Schoukens, *System Identification: A Frequency Domain Approach*. New York: IEEE Press, 2001.
- [19] P. Pisu, E. Silani, G. Rizzoni, and S. M. Savaresi, "A LMI-based supervisory robust control for hybrid vehicles," in *American Control Conf. 2003*, Denver, CO, pp. 4681–4686.
- [20] S. M. Savaresi, F. Taroni, F. Previdi, and S. Bittanti, "Control system design on a power-split CVT for high-power agricultural tractors," *IEEE/ASME Trans. Mechatronics*, vol. 9, no. 3, pp. 569–579, Sep. 2004.
- [21] S. M. Savaresi, R. Bitmead, and W. Dunstan, "Nonlinear system identification using closed-loop data with no external excitation: The case of a lean combustion process," *Int. J. Control*, vol. 74, pp. 1796–1806, 2001.
- [22] S. M. Savaresi, S. Bittanti, and M. Montiglio, "Identification of semi-physical and black-box non-linear models: The case of MR-dampers for vehicles control," *Automatica*, vol. 41, pp. 113–117, 2004.
- [23] S. M. Savaresi, H. Nijmeijer, and G. O. Guardabassi, "On the design of approximate nonlinear parametric controllers," *Int. J. Robust Nonlinear Control*, vol. 10, pp. 137–155, 2000.
- [24] S. M. Savaresi and B. Wittenmark, "Rejection of narrow-band disturbances subject to uncertain time-delays," *Int. J. Adapt. Control Signal Process.*, vol. 14, pp. 39–49, 2000.
- [25] A. V. Savkin and R. J. Evans, *Hybrid Dynamical Systems*. Cambridge, MA: Birkhäuser, 2002.
- [26] A. J. Scarlett, "Integrated control of agricultural tractors and implements: A review of potential opportunities relating to cultivation and crop establishment machinery," *Int. J. Comput. Electron. Agriculture*, vol. 30, no. 1–3, pp. 167–191, 2001.
- [27] M. Schwab, "Electronically-controlled transmission systems—Current position and future developments," in *Int. Congr. Transportation Electron.*, 1990, pp. 335–342.
- [28] P. Setlur, J. R. Wagner, D. M. Dawson, and B. Samuels, "Nonlinear control of a continuously variable transmission (CVT) for hybrid vehicle powertrains," in *IEEE/ASME Amer. Control Conf.*, 2001, vol. 2, pp. 1304–1309.
- [29] E. Silani, D. Fischer, S. M. Savaresi, E. Kaus, and R. Isermann, "Fault-tolerant filtering in active vehicle suspensions," presented at the FISITA 2004 World Automotive Congr., Barcelona, Spain, 2004.
- [30] E. Silani, S. M. Savaresi, S. Bittanti, A. Visconti, and F. Farachi, "The concept of performance-oriented yaw-control systems: Vehicle model and analysis," *SAE Trans., J. Passenger Cars—Mech. Syst.*, vol. 2002, pp. 1808–1818, 2003.
- [31] Y. Taguchi, A. Mineno, H. Kuzuya, Y. Soga, I. Horiuchi, Y. Ueda, and T. Miyazaki, "Development of an automated manual transmission system based on robust design," presented at the SAE 2003 World Congr. & Exhibition, Detroit, MI, Mar. 2003, Paper SAE 2003-01-0592.
- [32] H. Tanaka, "Speed ratio control of a parallel layout double cavity half-toroidal CVT for four-wheel drive," *J. Soc. Automotive Eng. Jpn.*, vol. 23, no. 3, pp. 213–217, 2002.
- [33] K. Wonoh and G. Vachtsevanos, "Fuzzy logic ratio control for a CVT hydraulic module," in *IEEE Int. Symp. Intell. Control*, 2000, pp. 151–156.
- [34] Q. Zheng, K. Srinivasan, and G. Rizzoni, "Dynamic modeling and characterization of transmission response for controller design," presented at the Int. Congr. Expo., Detroit, MI, Feb. 1998, Paper SAE 981094.
- [35] Q. Zheng and K. Srinivasan, "Transmission clutch pressure control system: Modeling, controller development and implementation," presented at the SAE 2000 World Congr., Detroit, MI, Mar. 2000, Paper SAE 2000-01-1149.
- [36] Z. Zou, Y. Zhang, X. Zhang, and W. Tobler, "Ratio control of traction drive continuously variable transmissions," in *IEEE/ASME Amer. Control Conf.*, 2000, vol. 3, pp. 1525–1529.



Sergio M. Savaresi (M'00) was born in Manerbio, Italy, on September 21, 1968. He received the M.Sc. degree in electrical engineering from Politecnico di Milano, Milan, Italy, in 1992, the Ph.D. degree in systems and control engineering from Politecnico di Milano, Milano, Italy, in 1997, and the M.Sc. degree in mathematics from the Università Cattolica, Milano, Italy, in 2002.

In 1998, he was with McKinsey & Co. In 1999, he joined Politecnico di Milano, where he is currently an Associate Professor in Automatic Control. He has been a Visiting Researcher at Lund University, Sweden; University of Twente, The Netherlands; Canberra National University, Australia; and Minnesota University, Minneapolis. His research interests include the areas of vehicles control, automotive systems, data analysis and system identification, nonlinear control theory, and control applications.

Dr. Savaresi serves as the Associate Editor of the *European Journal of Control*.



Mara Tanelli (M'05) was born in Lodi, Italy, in 1978. She received the Laurea degree in computer science engineering from Politecnico di Milano, Milan, Italy, in 2003 and the M.Sc. degree in computer science from the University of Illinois, Chicago, in 2003. She is currently pursuing a Ph.D. degree in information engineering at Politecnico di Milano.

Her research interests focus on automotive control systems and switched linear systems.



Francesco L. Taroni was born in Milan, Italy, on September 26, 1964. He received the M.Sc. degree in electronic engineering from Politecnico di Milano, Milan, Italy, in 1992.

In 1992, he was with the the R&D group, Esaote S.p.a., as the Designer of HW and SW for ultrasound digital ecographic systems. In 1997, he joined the SAME Deutz Fahr Group S.p.a., Bergamo, Italy, where he is currently with the Electrical and Electronic Department. His main job is to design the control of powertrain in tractor applications.



Fabio Previdi was born in Milan, Italy, on August 22, 1968. He received the "Laurea" degree (M.Sc.) in electronic engineering and the Ph.D. degree in computer science and automatic control from Politecnico di Milano, Milan, Italy, in 1993 and 1999, respectively.

From 1999 to 2001, he was a Research Assistant in automatic control at the Department of Electronics and Information Sciences, Politecnico di Milano, where he was also a Teaching Assistant for the courses of automatic control. From 1999 to 2000, he was a Visiting Scientist at the Center for Systems and Control, University of Glasgow, Scotland. From 1999 to 2001, he was a Contract Professor at the University of Bergamo, Bergamo, Italy. Since 2002, he is a Researcher at the University of Bergamo, where he teaches automatic control and industrial automation. In the past years, he has been involved in many national and international research projects developed by universities and industrial companies. He has published more than 40 papers in international journals and international conference proceedings. His research interests include fault diagnosis, nonlinear identification and control, LPV systems, application of control in biomedical engineering, and marine systems.



Sergio Bittanti (M'87-SM'98-F'01) received the Laurea degree in electronic engineering from the Politecnico di Milano, Milan, Italy, in 1970. He was a Project Manager of the Italian research network model identification, system control and signal processing, which connected about 70 Italian professor and researchers from various universities during 1988–1995. From 1993 to 1998, he coordinated the Ph.D. program in Computer and Control Engineering at Politecnico di Milano, Milan, Italy, where he is currently is a Professor in the Faculty of Engineering.

Besides being actively involved in various theoretical topics of system identification and control, he has also developed a number of advanced application studies in cooperation with industries. The outcomes of this intense research activity are summarized in hundreds of refereed papers in the best international journals. He is the author of a number of textbooks in Italian and the Editor Coeditor of four volumes in English (all published by Springer-Verlag). He is the Coeditor of *Identification, Adaptation, Learning—The Science of Learning Models From Data* (Berlin: Springer-Verlag 1996), which contains a collection of selected lectures given at the NATO ASI From Identification to Learning, Como, Italy, 1994.

Mr. Bittanti has served as an Editor for a number of journals and is currently the Editor-in-Chief of the *European Journal of Control*. He is a member of the IFAC Council. He has organized a number of conferences, the latest one being the IFAC Symposium on Robust Control, held in Milan, 2003.